Medical Engineering and Physics 117 (2023) 104003

Contents lists available at ScienceDirect

Medical Engineering and Physics

journal homepage: www.elsevier.com/locate/medengphy

Ex vivo experimental strategies for assessing unconstrained shoulder biomechanics: A scoping review

Jeremy Genter [a,b,c,*], Eleonora Croci [b,c], Hannah Ewald [d], Andreas M. Müller [c], Annegret Mündermann [b,c,e], Daniel Baumgartner [a]

[a] IMES Institute of Mechanical Systems, Zurich University of Applied Sciences ZHAW, Winterthur, Switzerland
[b] Department of Biomedical Engineering, University of Basel, Basel, Switzerland
[c] Department of Orthopaedics and Traumatology, University Hospital Basel, Basel, Switzerland
[d] University Medical Library, University of Basel, Basel, Switzerland
[e] Department of Clinical Research, University of Basel, Basel, Switzerland

A B S T R A C T

Background: Biomechanical studies of the shoulder often choose an *ex vivo* approach, especially when investigating the active and passive contribution of individual muscles. Although various simulators of the glenohumeral joint and its muscles have been developed, to date a testing standard has not been established. The objective of this scoping review was to present an overview of methodological and experimental studies describing *ex vivo* simulators that assess unconstrained, muscular driven shoulder biomechanics.
Methods: All studies with *ex vivo* or mechanical simulation experiments using an unconstrained glenohumeral joint simulator and active components mimicking the muscles were included in this scoping review. Static experiments and humeral motion imposed through an external guide, e.g., a robotic device, were excluded.
Results: Nine different glenohumeral simulators were identified in 51 studies after the screening process. We identified four control strategies characterized by: (a) using a primary loader to determine the secondary loaders with constant force ratios; (b) using variable muscle force ratios according to electromyography; (c) calibrating the muscle path profile and control each motor according to this profile; or (d) using muscle optimization.
Conclusion: The simulators with the control strategy (b) ($n = 1$) or (d) ($n = 2$) appear most promising due to its capability to mimic physiological muscle loads.

1. Introduction

The glenohumeral joint is one of the most complex joints in the human body. The incongruency of the smaller glenoid fossa compared to the large condyle of the humerus facilitates a large range of motion but also makes the glenohumeral joint prone to instability. To provide joint stability, various active (e.g. rotator cuff muscles) and passive (e.g. glenohumeral capsule) tissues are involved that must be considered when investigating glenohumeral biomechanics [1].

Previous studies have investigated the role of different factors contributing to glenohumeral stability and load, such as anatomy, muscle force, motion pattern, or pathology. Because joint load cannot be measured noninvasively in the living human, previous studies have used *ex vivo* approaches with shoulder simulators [2,3] or *in silico* methods such as musculoskeletal modelling approaches [4,5]. Shoulder simulators have been used to study passive biomechanics of the shoulder, such as joint stability due to joint reaction forces and joint concavity [6], stability of the glenohumeral capsule [7], and overall stability during specific movements (e.g. abduction and late cocking phase) [8]. Other groups investigated the role of muscles in glenohumeral biomechanics. To mimic the forces exerted by muscles, various shoulder simulators have been developed [9–11]. These simulators allow to test surgical interventions (e.g., rotator cuff tear repair) or the influence of prosthesis design (e.g., reverse shoulder arthroplasty (RSA)) on shoulder biomechanics to be investigated.

Although to date a standard defining the design and technical requirements is lacking, most simulators agree in their basic design. This comprises a clamping mechanism for the scapula and a pulley system attached to the tendon inserting into the humerus. Generally, shoulder simulators differ in three main aspects: the number of cables to mimic the studied muscles, the degrees of freedom (DoF) of the modelled joints, and the way the muscles are actuated. Existing simulators can be further categorized based on the technical solution utilized to generate the muscle forces. The most trivial simulators load the muscle pulley with passive loads such as springs or simple counterweights, more advanced simulators use active actuators such as pneumatic cylinders or motors to mimic increasing muscle forces with increasing abduction angles [12]. To our best knowledge, Williamson et al. [12] performed the only

* Corresponding author: ZHAW School of Engineering, IMES, Technikumstrasse 71, Winterthur 8401, Switzerland.
E-mail address: gent@zhaw.ch (J. Genter).

https://doi.org/10.1016/j.medengphy.2023.104003
Received 15 January 2023; Received in revised form 22 May 2023; Accepted 27 May 2023
Available online 28 May 2023

systematic review of *ex vivo* experiments. Specifically, they investigated experiments regarding rotator cuff tears and instability. Although they identified various experimental setups, few of the included studies used dynamic muscle forces. Furthermore, they divided the *ex vivo* experiments into three main topics: shoulder joint orientation and mobility; muscle activation and humeral motion; and influence of glenohumeral capsule condition. Two of the most important findings of the review [12] were that the rotator cuff muscles are mostly statically loaded and that only a few simulators load the rotator cuff muscles dynamically.

Despite lacking precision of anatomical representation or physiological muscle recruitment, these simulators are used to answer research questions ranging from joint implant loading [2] to the effect of rotator cuff muscle activation on glenohumeral kinematics [11] to joint reaction forces during daily activities [13]. Williamson et al. [12] focused their search on experimental setups for rotator cuff repair and instability and not on dynamic and unconstrained motions of the glenohumeral joint simulators, thus the most advanced and physiological simulators were underrepresented in their review.

In this scoping review, we focused our search on experiments with active glenohumeral joint simulators, hence extending the review by Williamson et al. [12]. Specifically, we provide an overview of the approaches to design unconstraint simulators, and describe differences and commonalities of *ex vivo* glenohumeral experimental setups of simulators including their strengths and limitations.

2. Materials and methods

This scoping review was conducted in accordance with the Joanna Bricks Institute methodology for scoping reviews [14] and followed the PRISMA reporting guideline [15].

2.1. Search

Text words with synonyms and word variations as well as subject headings in the topics *ex vivo*, simulator, shoulder muscles and biomechanics were used by a medical information specialist (HE) to conduct a search in the databases PubMed, Embase via Elsevier and the Web of Science Core collection. We previously published the study protocol with the detailed search strategy [16,17]. The search was conducted on 12 July 2021. Articles published later were not included in this scoping review.

In contrast to the protocol, citation tracking was not fully conducted. Based on the included articles, we conducted backward and forward citation tracking using the citation chaser tool [18]. However, a test screening of 100 abstracts of the 2838 newly found articles with citation tracking did not result in any additional information on simulator setups. Revisiting our search strategy, we are confident that all currently available simulator setups were found. Therefore, we decided to not pursue citation tracking any further.

2.2. Eligibility criteria

We included studies if the described simulator induced the continuous motion through an actuator of muscle forces comprising at least three distinct actuators, at least one of which had to be for the deltoid muscle and one for the rotator cuff muscles. Studies were excluded if the glenohumeral motion was constrained by other than its anatomical structures or implants, if the motion was passive (e.g., guided externally with a robotic device), or if performed with animal samples.

2.3. Study selection

Two reviewers (JG, EC) independently screened titles and abstracts. Potentially pertinent articles were retrieved as full-text and again screened independently. Any disagreement between reviewers regarding eligibility was resolved in discussion with an additional reviewer (DB).

2.4. Study synthesis / analysis

We qualitatively summarized the extent of the simulators using five categories: (i) mechanical aspects of the shoulder simulator; (ii) sensors used; (iii) research question; (iv) specimen preparation; and (v) control strategies, since all studies used different methodologies. In category (i) the mechanical concept was summarized including how and how many muscles are actuated. In category (ii) we were interested in the measurements performed for the data acquisition and for the feedback control. In category (iii), we presented what kind of studies were performed with these simulators. In category (iv), we presented what of the specimen was used and how they were prepared. In category (v), the control strategies are presented. As the glenohumeral joint is an underdeterministic system (i.e., a system with more muscles than DoF) we elaborated on the researcher's strategy to solve this problem.

3. Results

The electronic database search and removal of duplicates yielded 3439 abstracts, and the abstract screening yielded 141 eligible papers for the full text screening (Fig. 1). After full text screening, 51 papers were included. These papers were grouped according to specific simulators yielding nine distinct simulators (Fig. 2).

Because multiple studies were found for most simulators, an identification number (S) was assigned to each simulator (Table 1).

3.1. Mechanical aspects of the shoulder simulator

All simulators followed the same principle for designing the active muscle forces. The muscle forces are induced by actuators through a pulley system to the insertion site of the muscles on the humerus. The pulleys are adjusted to recreate the line of action of each muscle. Five simulators (S1, S3, S4, S6, S8 [2,10,19–35]) use electromotors to actuate the glenohumeral joint. The other simulators use either hydraulic cylinders (S2 and S9) [3,36–55] or pneumatic cylinders (S5 and S7 [22–29, 56]). The design of all simulators allows 6 DoF in the glenohumeral joint. Four simulators (S1, S3, S5, S8 [2,9,10,19–21,34,35,57–64]) have an additional DoF to rotate the scapula in the scapular plane.

The simulators vary in their use of active (actuated) and passive (e.g., loaded with springs and weights) muscles. The number of active muscles ranges from four to eight. While most simulators do not use any passive muscles, Dyrna et al. [22–29] (S4) loaded the infraspinatus and subscapularis muscles with constant weights, and Payne et al. [56] (S7) created a passive load of the biceps muscle via a static pressure in a pneumatic cylinder. The middle portion of the deltoid muscle is included in all simulators, whereas the anterior and posterior portion of the deltoid is used in six of nine simulators (S1, S2, S4, S6, S7, S9 [2,3, 22–33,36–45]). The rotator cuff muscles (supraspinatus, infraspinatus, and teres minor muscles) are included in all simulators, but the infraspinatus and the teres minor muscles were always combined as a single muscle. The pectoralis major and latissimus dorsi muscles are used as active muscles in four simulators (S1, S3, S5, S6 [2,9,19,21,30–33, 46–64]). For S1 [2] seven actuators were specified, but eight muscles are reported in their results section.

3.2. Sensors

Five simulators (S1, S3–6 [2,9,19,22–33,57–64]) measure the kinematics using an optical tracking system. However, S3 uses an optical tracking system only in the study of Bouaicha et al. [19] for measuring humeral head translations, but glenohumeral joint angles are measured using a 6 DoF inertial measurement unit [10,19–21]. The simulator S2 [3,36–45] tracks the 6 DoF of the glenohumeral joint using a magnetic tracking device. S7 [56] measures the angular position of the

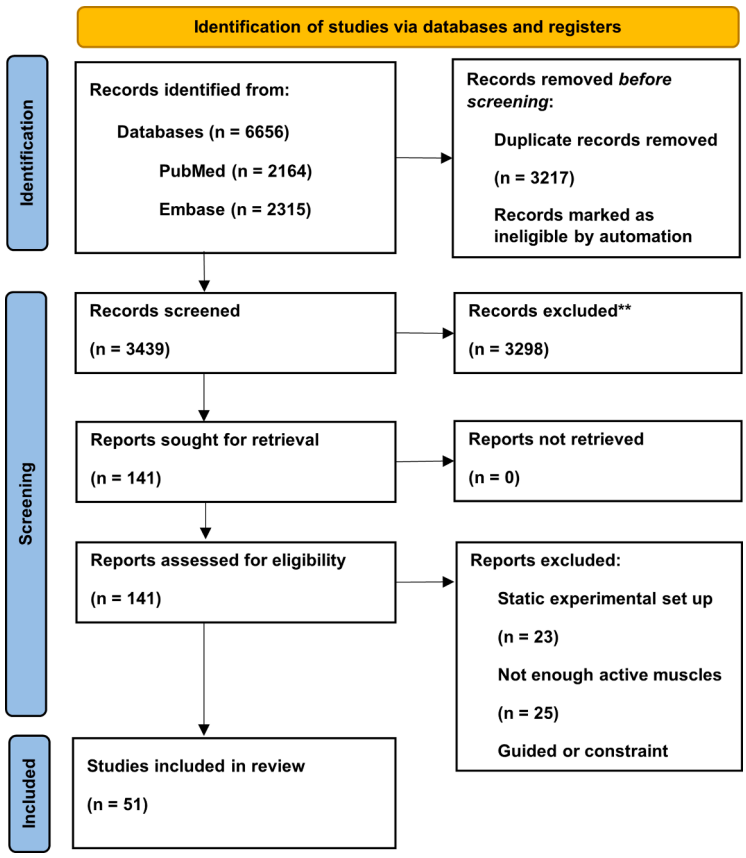

Fig. 1. Flow diagram for the scoping review process according to the PRISMA statement (2020).

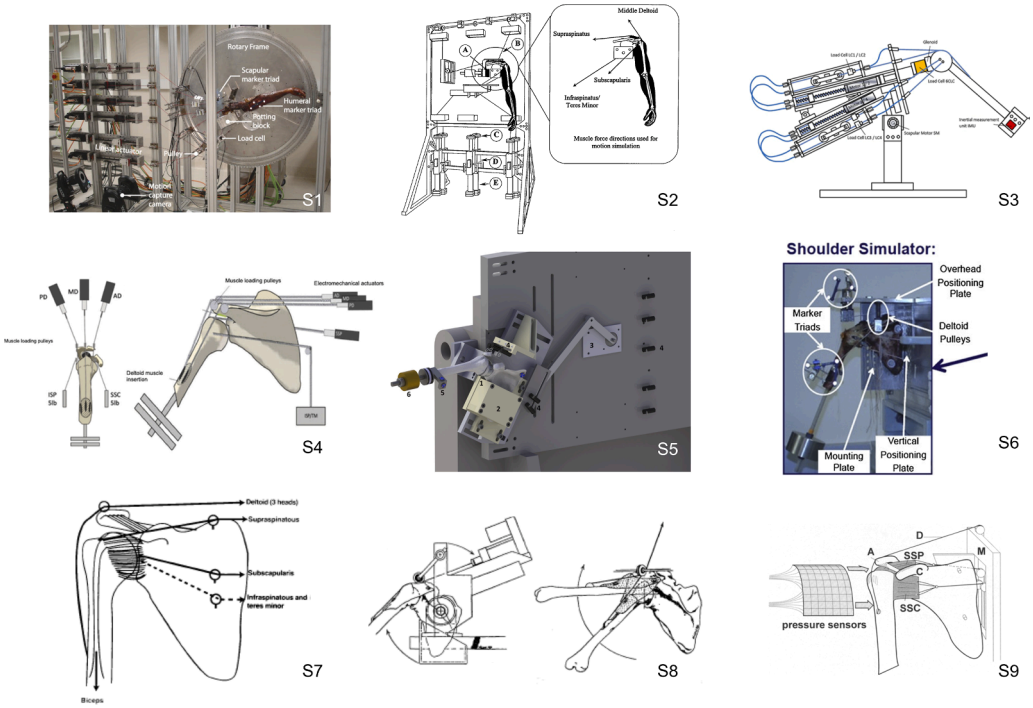

Fig. 2. Illustrations of the simulators. Please see the note at the end of the paper, containing license details for figure reuse.

glenohumeral joint using a rotation gauge. S8 [34,35] determines the angular position of the glenohumeral joint using the actuator position of the deltoid muscle and the scapular motor position to measure the scapular abduction. S9 [46–55] measures the glenohumeral kinematics using six ultrasonic tracking devices. For S4 [22,26,27,29] it was explicitly reported that the actuator positions were measured.

Table 1
Overview of experimental shoulder simulators. Legend: DELTA—anterior deltoid; DELTM—middle deltoid; DELTP—posterior deltoid; SSP—supraspinatus; ISP—infraspinatus and teres minor; SSC—subscapularis; PM—pectoralis major; LD—latissimus dorsi; CSA—critical shoulder angle; EMG—electromyography; RSA—reverse shoulder arthroplasty; SA—shoulder arthroplasty.

General				Mechanical System					Control System		
ID	Country	Specimen type	Research Question	DoF	Active muscles	Passive muscles	Muscle insertion	Measurements	Sensors	Control strategy	Motion
S1[2]	Australia	Fresh frozen cadaveric shoulders	Biomechanics after RSA	7	DELTA, DELTM, DELTP, SSP, ISP, SSC, PM, LD	None	Anatomical sites on the cadaver	Muscle-, joint forces, kinematics	6-Camera optical tracking system (kinematics), universal joint force sensor (joint load), load cells (muscle forces)	2:1 scapulo-humeral rhythm; pre-estimated muscle froces	Abduction / flexion
S2[3,36–45]	USA	Fresh frozen cadaveric shoulders	Capsule injury biomechanics, general shoulder biomechanics, simulator validation, rotator cuff tear	6	DELTA, DELTM, DELTP, SSP, ISP, SSC	None	Anatomical sites on the humerus, scapular muscle origins are estimated from a prior conducted MRI	Muscle-, joint forces, kinematics	Magnetic tracking device (kinematics), universal joint force sensor (joint load), load cells (muscle forces)	Constant muscle force ratio	Abduction / external and internal rotation
S3[10,19–21]	Switzerland	Thiel-fixed cadaveric shoulders	Simulator validation, CSA	7	DELTM, SSP, ISP, SSC, PM, LD	None	Anatomical sites on the humerus, scapular origin fixed except deltoid origin, deltoid origin is varied to change the CSA	Muscle-, joint forces, kinematics	IMU (joint angles), optoelectronic motion capture system (joint translations), 6-axis load cell (joint forces), load cells (muscle forces)	2:1 scapulo-humeral rhythm; Constant muscle force ratio	Abduction
S4[22–29]	USA	Fresh frozen cadaveric shoulders	Capsule injury biomechanics, rotator cuff tear, biomechanics after SA	6	DELTA, DELTM, DELTP, SSP	ISP, SSC	Anatomical sites on the humerus, estimated from scapular bony landmarks	Muscle-, joint forces, kinematics, actuator position	Optical tracking system and live fluoroscopy (kinematics), load cells (muscles forces), actuator position	Calibrated motion profiles of each actuator	Abduction
S5[9,57–64]	Canada	Fresh frozen cadaveric shoulders	Biomechanics after RSA, rotator cuff tear, general shoulder biomechanics, simulator validation	7	DELTM, SSP, ISP, SSC, PM, LD	None	Anatomical sites on the humerus, deltoid origins are adjusted until the EMG based ratios resulted in scapular-plane abduction	Muscle-, joint forces, kinematics	Optical tracking system (kinematics), load cell in RSA (joint force), air pressure sensor (muscles forces), load cell (deltoid muscle)	Variable scapulo-humeral rhythm; EMG based muscle ratios with three individual PID Controllers	Abduction / flexion / external and internal rotation
S6[30–33]	USA	Fresh frozen cadaveric shoulders	Biomechanics after RSA, rotator cuff tear	6	DELTA, DELTM, DELTP, SSP, ISP, SSC, PM, LD	None	Anatomical sites on the humerus, scapular muscle origins not reported	Muscle-, joint forces, kinematics	Optical tracking system (kinematics), load cells (muscle forces)	Real time static muscle optimization	Not reported
S7[56]	USA	Fresh frozen cadaveric shoulders	Impingement syndrome	6	DELTA, DELTM, DELTP, SSP, ISP, SSC	Long head of the biceps	Anatomical sites on the humerus, deltoid origins are adjusted until the EMG based ratios resulted in scapular-plane abduction	Muscle-, joint forces, kinematics, pressure under coracoacromial arch	Rotational gauge (internal / external rotation and elevation), load cells (muscle forces), 5 pressure transducer (coracoacromial arch pressure)	EMG based muscle force ratios	Abduction
S8[34,35]	USA	Fresh frozen	Rotator cuff tear, general	7	DELTM, SSP, ISP, SSC	None	Anatomical sites on the cadaver	Muscle-, joint forces,	Deltoid actuator and scapula actuator position	1.5:1 1 scapulo-humeral	Abduction

(*continued on next page*)

Table 1 (*continued*)

General ID	Country	Specimen type	Research Question	Mechanical System DoF	Active muscles	Passive muscles	Muscle insertion	Measurements	Control System Sensors	Control strategy	Motion
		cadaveric shoulders	shoulder biomechanics					kinematics, length of deltoid	(abduction and scapula rotation), force transducers (muscle forces)	rhythm; position control of the deltoid	
S9[46–55,65]	Germany	Fresh frozen cadaveric shoulders	Impingement syndrome, capsule injury biomechanics, general shoulder biomechanics,	6	DELTA, DELTM, DELTP, SSP, ISP, SSC	None	Anatomical sites on the humerus, scapular muscle origins are estimated from a prior conducted MRI	Muscle-, joint forces, kinematics, pressure sensor at coracoacromial arch	6 ultrasonic sensors (kinematics), load cells (muscle forces)	Constant muscle force ratio	Abduction

S1–S3, and S5 [2,3,10,19–21,38–41,43,44,59,60,64] measure the glenohumeral joint forces using a universal force/moment sensor. However, only in three studies [59,60,64] on S5, an integrated sensor in the implanted RSA was used to measure the joint forces. Eight simulators (S1–S4, S6–S9 [2,3,10,19–56]) measure the actuator forces using force cells. The developers of S5 reported one force cell for the middle portion of the deltoideus muscle [9] and stated that the pneumatic actuators were pressure-controlled [57].

S7 [56] measures the coracoacromial arch pressure using five pressure sensors, whereas S9 uses 168 capacitive pressure sensors to measure the pressure in the coracoacromial arch [49,51,52].

3.3. Research question

Of the 51 studies, 14 investigated rotator cuff tears [23–27,32,34,39,40,44,45,60,62,63], 13 the general biomechanics of the glenohumeral joint [3,9,35,38,41,42,47,48,53–55,61,65], eight the biomechanics after RSA [2,30,31,33,57,59,60,64], five the glenohumeral capsule injury [22,29,36,43,46], six the impingement under the coracoacromial arch [49–52,56,65], three the critical shoulder angle [19–21], one the biomechanics after anatomical shoulder arthroplasty [28] and four validated their simulator [10,37,57,58].

3.4. Specimen preparation

Overall, 49 studies used cadaveric specimens, of which two studies [19,21] used Thiel's fixation method to conserve the cadaveric tissue and all others used fresh frozen cadaveric shoulders. Two studies used a metallic dummy as humerus and a polyethylene dummy as glenoid [10,20].

While in general the specimens were dissected and the tendon insertion at the humerus as well as the capsular complex were left intact, some individual differences in specimen preparation amongst studies were present. The studies conducted on S1 [2] and S2 [3,36–45] removed mainly soft tissue proximal to the glenohumeral joint and the muscle tissue of the muscles to be simulated leaving only the tendon insertion intact. All other studies dissected the humerus distal to the insertion of the deltoid muscle. This led to a loss of the arm weight which was then replaced with a concentrated mass ranging from 1.7 kg [22] to 3.5 kg [30,31] at an estimated centre of mass ranging from 30 cm [10,21–29] to 31.5 cm [30]. The studies using S5 [9,57–64] did not report the mass added to the humerus. Moor et al. [21] and Bouaicha et al. [19] (S3) removed the capsule to separate the scapula from the humerus. To study the capsule, Apreleva et al. [36] (S2) created a Bankart lesion artificially, whereas Hurschler et al. [46] (S9), McMahon et al. [43] (S2) and Scheiderer et al. [29] (S4) created a capsule lesion artificially. In nine studies [2,28,30,31,33,57,59,60,64] (S1, S4-S6), total shoulder arthroplasty was performed.

The scapula of S2 and S4 is mounted in a 6-DoF mounting jig [22-26,28,29,37,40,42]. In S3 the glenoid inclination could be adjusted [19]. The researcher using S5 mounted the scapula rigidly with a 10° upwards inclination of the glenoid [57,59,60,64]. The researchers of S6, S7 and S9 mounted the scapula rigidly into the simulator with 10° ventral inclination and the margo medials was aligned with the vertical axis [30–32,46–56,65]. Whereas the researchers of S1 and S8 did not report how they orientated the scapula in the simulator.

3.5. Control strategy

Various control strategies were employed. The most common strategy was to use a constant ratio to share the load between muscles. Baumgartner et al. [10]. used a prime loader, the deltoid muscle, to initiate abduction (S3). The deltoid is driven by the abduction angle controlled with a proportional, integral, and derivative (PID) controller. The supraspinatus muscle is loaded by a constant ratio proportional to the load of the deltoid muscle. The infraspinatus muscle is controlled by a position PID controller of the internal/external rotation of the humerus, whereas the subscapularis muscle is controlled by a force controller which uses the mean loads of the subscapularis and infraspinatus muscles as feedback. The pectoralis major and infraspinatus muscles are loaded by an electromyography (EMG) based activation ratio in relation to the abduction angle taken. Other developers used a similar approach where all muscles are loaded with a constant ratio, but the muscle force ratios differed amongst studies (S2, S7-S9 [3,35,36,42,45,54,56]). In one of the simulators, the developers extended this strategy to variable EMG based ratios (S5) [9,66]. The EMG patterns were derived from Kronberg et al. [67]. In later studies, Giles et al. [57,58] improved this simulator even further and implemented a multi-parallel PID controller. Each DoF is controlled by one PID controller. The primary PID controller evaluates the desired forces to abduct the humerus and determines the resultant force of the three deltoid segments. The sums based on the variable EMG based ratios [9,66] (plane of abduction DoF: sum of the anterior and posterior portion of the deltoid muscle; axial rotation DoF: sum of the subscapularis and infraspinatus/teres minor muscles) multiplied by the resultant force of the deltoid are used as input for the secondary PIDs (abduction plane and internal rotation). These PIDs reapportioned the total applied muscle force to their controlled muscles. Lastly, a PID is implemented to control the rotation of the scapula with a direct current (DC) motor.

Dyrna et al. [26,27] abducted the humerus to its target value to calibrate each muscle force at the target abduction (S4). For the actual test, a preload of the muscles was applied and then increased linearly until the force at the target abduction was achieved. Two simulators (S1, S6 [2,30,31]) estimate the muscle forces using a musculoskeletal model.

Ackland et al. [2]. estimated the muscle forces a priori, whereas Gulotta et al. [30,31] implemented a real time optimizer that estimates the muscle forces needed to move the humerus. This optimizer uses a static muscle optimization technique minimizing the sum of the cubed muscle stresses.

4. Discussion

We described existing unconstrained simulators that can be considered the most advanced simulators as they overcame the most prominent simplification of constraining the motion or guiding the motion. The mimicking muscles are an essential part of unconstrained simulators to ensure stability and motion in the joint. While the rotator cuff muscles and the middle deltoid muscle are at least incorporated in all simulators, none of the reported simulators included the biceps, triceps, teres major or the coracobrachialis muscles as active muscles. S1 [2] and S6 [30–33] had the most muscles (eight). All simulators represented the rotator cuff muscles and at least one segment of the deltoid muscle. The number of muscles to be represented in a glenohumeral simulator remains open and depends on the specific research question. Although several studies have advanced our insight into the role of muscles for joint motion and stabilization, [68,69] the consideration of muscular activity in general remains highly debated [70]. Kian et al. [71] compared static muscle optimization to EMG based optimization and showed that the activity of antagonistic muscles is underestimated. Thus, adding antagonistic muscles to the simulators increases its physiological significance in most research questions regarding glenohumeral joint mechanics.

Most glenohumeral simulators in our review recreated only the motion of the humerus, where the scapula is assumed to be fixed. Only few simulators (S1, S3, S5, S8 [2,9,10,19-21,34,35,57–64]) incorporated the scapular motion, which is restricted within the scapular plane. Already in the 1940s, Inman et al. [72] observed an average scapulohumeral rhythm of 2:1 (humeral to scapular motion) after 30° of abduction or 60° of flexion. McQuade and Smith [73] evaluated a non-linear scapulohumeral rhythm with a dependence on shoulder load. This is a major limitation in all presented simulators. None of the simulators go beyond the scapulohumeral rhythm of 2:1. The scapular position affects the joint reaction force in the glenoid even if only the gravitational force of the humerus is considered. Furthermore, most simulators restrict humerus motion to abduction in the scapular plane, whereas only S1, S2 and S5 reported an expansion of the motion of the humerus to flexion, internal rotation, and flexion and internal rotation, respectively.

All simulators used at least one sensor to determine the kinematics of the glenohumeral joint and all simulators measured the muscle forces. Some simulators measured joint reaction forces (S1–3, S5 [2,3,10, 19–21,38–41,43,44,59,60,64]) while others measured joint contact pressures (S7 [56] and S9 [49,51,52]). However, the joint contact pressures were only measured in the coracoacromial vault since the sensors do not fit into the glenohumeral spacing and would alter the mechanics within the joint.

To relate the measurements of the simulators as closely as possible to a native anatomical setting, they all were used at least once in an *ex vivo* study. Regarding specimen preparation, two main approaches were pursued: either as little or as much as possible was dissected. For instance, the studies conducted on S1 [2] and S2 [3,36–45] removed only the soft tissues proximal to the glenohumeral joint and the simulating muscles. With this approach the specimen-specific mass distribution was kept mostly intact. The other approach left only the muscle insertion intact and compensated for the lost arm mass by attaching an additional weight. Other variations in preparation were mostly due to the nature of the study question (e.g., condition of the glenohumeral capsule, implants, and rotator cuff repair).

Overall, the mechatronic design of glenohumeral simulators requires actuation for the transmission of musculotendinous forces, sensors to detect the current state, and inclusion of the most relevant native tissue to mimic the *in vivo* situation. Electromotors are often used for muscle actuation because they have high accuracy and short system response time. However, they have limited force output. In contrast, pneumatic actuators can generate higher force output, and hydraulic actuators can produce even higher forces. They are also simple in design, but require a supply of compressed air or hydraulic fluids. This compressor or pump can be placed separately next to the simulator.

Measuring kinematics using optical, magnetic, or ultrasonic tracking devices provides good accuracy. However, each of these methods also has disadvantages. Optical tracking devices require a clear view on the markers [2,9,19,22–33,57–64]. Magnetic tracking devices are sensitive to electromagnetic interference, so consideration must be given to using them with electromotors [3,36–45]. Ultrasonic tracking devices have a limited range, and thus placement of the sensors must be carefully chosen [46–55]. Rotational gauges [56] and inertial measurement units [10,19–21] are inexpensive and easy to integrate into the control system, but they are less accurate and cannot measure translation. Measuring joint position via only the position of the muscle actuator can be challenging, depending on the compliance of the cable pulley and the dynamic forces involved [22,26,27,29].

Joint reaction forces can be measured with 6-DoF force cells, but placement must be considered to avoid interference with the native tissue of the joint. Muscle forces should be measured in the cable pulley system with force cells to obtain accurate measurements. Coracoacromial pressure can be measured with pressure sensors, but the sensors should be as thin as possible to minimize measurement interference.

The control strategy is of utmost importance for approximating a physiological behavior. We identified four principles of control strategy to achieve this: (a) using a primary loader to determine the secondary loaders with constant force ratios, (b) using variable muscle force ratios according to EMG patterns, (c) calibrating the muscle path profile and control each motor according to this profile and (d) using muscle optimization. Of those four principles, (a) is the most used and apparently the least complex to implement in such an under-deterministic system of muscles. Principle (b) exploited the potential of principle (a) to its fullest and was validated to be highly repeatable [57,58]. Even though the EMG data provides a more physiological muscle force pattern than in principle (a), the EMG data has to be specific for each motion and pathology [74,75]. Principle (c) was used only in S4. The disadvantage of using a position-controlled setting in an under-deterministic system of muscles is that the muscle forces are most likely determined by the stiffness of the pulley system. A change in stiffness would result in different muscle force loadings (e.g., surgical repair of the rotator cuff, different length of the pulley cable, different material in the system, etc.). Principle (d) makes use of muscle optimization. S1 [2] estimates the muscle optimization a priori, and S6 [30,31,33] uses a real time optimizer to determine the muscle loads. However, no details are provided on how the error control is designed. A real time optimizer based on a musculoskeletal model seems to have promising potential, but our research revealed no studies on the validation of these simulator types.

For future generations of physiological glenohumeral simulators, we recommend that researchers incorporate scapular motion, improve muscular load transmission, carefully consider the control strategy, and include as much soft tissue as the design allows. Scapular motion may influence muscular load during arm abduction or elevation and provide compensatory mechanisms in pathologies. Implementation of the deltoid muscle as several separate segments should be reconsidered because muscle wrapping over the bones differs from the *in vivo* situation. Furthermore, we recommend implementing a control strategy that more closely resembles the physiological situation, such as EMG-based control or muscle optimization validated against EMG patterns. However, it should be noted that EMG can be influenced by pathology and/or bone morphology. In addition, we anticipate that preserving the integrity of the soft tissue, particularly the capsule, is crucial, as it may impact the translation of the glenohumeral joint upon the release of

intracapsular pressure.

This review of existing *ex vivo* shoulder simulators is also relevant in the context of glenohumeral finite element models. To date, finite element models have not been compared or combined with *ex vivo* experimental simulators. Experimental data obtained in physiological shoulder simulators may be used to select and design an appropriate finite element model, compare their results directly with *ex vivo* measurements and hence provide a validation framework for these models.

We limited the search in this study to unconstrained, muscular controlled glenohumeral simulators, which excluded many other *ex vivo* glenohumeral experimental setups. This may have excluded other mechanical setups with different preparation methods, sensors, and control strategies.

5. Conclusions

Various active, muscular controlled simulator designs have been reported that mainly differ in their control strategy and scapular motion. Here, three simulators shall be highlighted (S1, S4 and S6) in regard of their control strategy. The control strategy of S4 is reported in detail, and S4 is the only simulator that incorporates position-dependent EMG data. S1 and S6 use musculoskeletal optimization to mimic the *in vivo* situation. Although documentation on the error control and validation with *in vivo* data is lacking, this strategy has a large potential for mimicking the physiological condition. In particular, a physiologic simulation is important as it mirrors the high variation of different, patient specific patterns that would also be present in real patient groups. Overall, the overview of different control strategies and the inclusion of the scapular motion for simulating the human shoulder ex vivo supports the understanding of physiological shoulder testing and may help in the design and development of future, more advanced simulators.

All current simulators approximate the *in vivo* situation and can only simulate pathologies and their treatment by considering all underlying assumptions and technical constraints. Further research, development, and validation are needed to use them as reliable and meaningful testing methods.

Funding

This project is funded by the Swiss National Science Foundation (SNF 189082). The funders had no role in the study design, data collection and analysis, decision to publish, or preparation of the manuscript.

Ethical approval

Not required.

Notes

S1 (reprinted from Journal Orthopaedic Research, Vol. 29 Issue 12, Muscle and joint-contact loading at the glenohumeral joint after reverse total shoulder arthroplasty, Pages 1850–1858, © 2011 Orthopaedic Research Society with permission from John Wiley and Sons); S2 (reprinted from Journal of Shoulder and Elbow Surgery, Vol. 9 Issue 5, Maria Apreleva, I.M. Parsons, Jon J.P. Warner, Freddie H. Fu, Savio L.-Y. Woo, Experimental investigation of reaction forces at the glenohumeral joint during active abduction, Pages 409–417, © 2000 by Journal of Shoulder and Elbow Surgery Board of Trustees with permission from Elsevier); S3 (reprinted by permission from Springer Nature Customer Service Centre GmbH: Springer Nature, Medical & Biological Engineering & Computing, D. Baumgartner, D. Tomas, L. Gossweiler, W. Siegl, G. Osterhoff and B. Heinlein, Towards the development of a novel experimental shoulder simulator with rotating scapula and individually controlled muscle forces simulating the rotator cuff, © International Federation for Medical and Biological Engineering 2013); S4 (reprinted from Arthroscopy: The Journal of Arthroscopic & Related Surgery, Vol. 26 Issue 2, Christopher R. Adams, Brendan Comer, Bastian Scheiderer, Florian B. Imhoff, Daichi Morikawa, Cameron Kia, Lukas N. Muench, Joshua B. Baldino, Augustus D. Mazzocca, The Effect of Glenohumeral Fixation Angle on Deltoid Function During Superior Capsule Reconstruction: A Biomechanical Investigation, Pages 400–408, © 2019 by the Arthroscopy Association of North America with permission from Elsevier); S5 (reprinted from J. W. Giles, G. D. Langohr, J. A. Johnson and G. S. Athwal, Implant Design Variations in Reverse Total Shoulder Arthroplasty Influence the Required Deltoid Force and Resultant Joint Load, Clinical Orthopaedics Related Research, 2015, Vol. 473, Issue 11, Pages 3615–3626 https://journals.lww.com/clinorthop/pages/default.aspx, © The Association of Bone and Joint Surgeons1 2015 with permission from Wolters Kluwer Health, Inc); S6 (reprinted from Journal of Shoulder and Elbow Surgery, Vol. 21 Issue 9, Lawrence V. Gulotta, Dan Choi, Patrick Marinello, Zakary Knutson, Joseph Lipman, Timothy Wright, Frank A. Cordasco, Edward V. Craig, Russell F. Warren, Humeral component retroversion in reverse total shoulder arthroplasty: a biomechanical study, Pages 1121–1127, © 2012 Journal of Shoulder and Elbow Surgery Board of Trustees, with permission from Elsevier); S7 (L. Z. Payne, X. H. Deng, E. V. Craig, P. A. Torzilli and R. F. Warren, American Journal of Sports Medicine (Vol. 25 Issue 6) pp. 801–808, copyright © 1997 by (SAGE Publications) reprinted by Permission of SAGE Publications); S8 (reprinted from Journal Orthopaedic Research, Vol. 12 Issue 5, The entire rotator cuff contributes to elevation of the arm, Pages 699–708, ©Orthopaedic Research Society (2005), with permission from John Wiley and Sons); S9 (reprinted from Journal of Shoulder and Elbow Surgery, Vol. 4 Issue 6, N. Wuelker, B. Roetman, S. Roessig, Coracoacromial pressure recordings in a cadaveric model, Pages 462–467, © 1995 by Journal of Shoulder and Elbow Surgery Board of Trustees with permission from Elsevier)

Declaration of Competing Interest

None declared

References

[1] Lugo R, Kung P, Ma CB. Shoulder biomechanics. Eur J Radiol 2008;68:16–24.
[2] Ackland DC, Roshan-Zamir S, Richardson M, Pandy MG. Muscle and joint-contact loading at the glenohumeral joint after reverse total shoulder arthroplasty. J Orthop Res 2011;29:1850–8.
[3] Apreleva M, IMt Parsons, Warner JJ, Fu FH, Woo SL. Experimental investigation of reaction forces at the glenohumeral joint during active abduction. J Shoulder Elbow Surg 2000;9:409–17.
[4] Nikooyan AA, Veeger HE, Westerhoff P, Graichen F, Bergmann G, van der Helm FC. Validation of the Delft Shoulder and Elbow Model using in-vivo glenohumeral joint contact forces. J Biomech 2010;43:3007–14.
[5] Anglin C, Wyss UP, Pichora DR. Glenohumeral contact forces. Proc Inst Mech Eng H 2000;214:637–44.
[6] Lippitt S, Matsen F. Mechanisms of glenohumeral joint stability. Clin Orthop Relat Res 1993:20–8.
[7] Billuart F, Devun L, Skalli W, Mitton D, Gagey O. Role of deltoid and passives elements in stabilization during abduction motion (0 degrees-40 degrees): an ex vivo study. Surg Radiol Anat 2008;30:563–8.
[8] Clabbers KM, Kelly JD, Bader D, Eager M, Imhauser C, Siegler S, et al. Effect of posterior capsule tightness on glenohumeral translation in the late-cocking phase of pitching. J Sport Rehabil 2007;16:41–9.
[9] Kedgley AE, Mackenzie GA, Ferreira LM, Drosdowech DS, King GJ, Faber KJ, et al. The effect of muscle loading on the kinematics of *in vitro* glenohumeral abduction. J Biomech 2007;40:2953–60.
[10] Baumgartner D, Tomas D, Gossweiler L, Siegl W, Osterhoff G, Heinlein B. Towards the development of a novel experimental shoulder simulator with rotating scapula and individually controlled muscle forces simulating the rotator cuff. Med Biol Eng Comput 2014;52:293–9.
[11] Williamson PM, Hanna P, Momenzadeh K, Lechtig A, Okajima S, Ramappa AJ, et al. Effect of rotator cuff muscle activation on glenohumeral kinematics: a cadaveric study. J Biomech 2020;105:109798.
[12] Williamson P, Mohamadi A, Ramappa AJ, DeAngelis JP, Nazarian A. Shoulder biomechanics of RC repair and Instability: a systematic review of cadaveric methodology. J Biomech 2019;82:280–90.
[13] Hughes DJ, Hodgson S, Nabhani F. Validation of a novel mechanical testing rig for investigating forces in the glenohumeral joint. Curr Orthop Pract 2012;23:140–5.

[14] Peters MDJGC, McInerney P, Aromataris EMZ. JBI manual for evidence synthesis. editor. Chapter 11: scoping reviews2020. 2023.
[15] Tricco A, Lillie E, Zarin W, O'Brien K, Colquhoun H, Levac D, et al. PRISMA Extension for Scoping Reviews (PRISMAScR): checklist and explanation. Ann Intern Med 2018;169:467–73.
[16] Genter J, Croci E, Ewald H, Müller A, Mündermann A, Baumgartner D. *Ex-vivo* experimental strategies for assessing unconstrained shoulder biomechanics: a scoping review protocol [version 3; peer review: 2 approved]. F1000Research 2023;11:77.
[17] Genter J, Croci E, Ewald H, Müller AM, Mündermann A, Baumgartner D. *Ex-vivo* experimental strategies for assessing unconstrained shoulder biomechanics: a scoping review\'s detailed search strategy. Zenodo; 2021.
[18] Haddaway NR, Grainger MJ, Gray CT. citationchaser: an r package and shiny app for forward and backward citations chasing in academic searching. 0.0.3 ed. Zenodo; 2021.
[19] Bouaicha S, Kuster RP, Schmid B, Baumgartner D, Zumstein M, Moor BK. Biomechanical analysis of the humeral head coverage, glenoid inclination and acromio-glenoidal height as isolated components of the critical shoulder angle in a dynamic cadaveric shoulder model. Clin Biomech 2020;72:115–21. Bristol, Avon.
[20] Gerber C, Snedeker JG, Baumgartner D, Viehöfer AF. Supraspinatus tendon load during abduction is dependent on the size of the critical shoulder angle: a biomechanical analysis. J Orthop Res 2014;32:952–7.
[21] Moor BK, Kuster R, Osterhoff G, Baumgartner D, Werner CM, Zumstein MA, et al. Inclination-dependent changes of the critical shoulder angle significantly influence superior glenohumeral joint stability. Clin Biomech 2016;32:268–73. Bristol, Avon.
[22] Adams CR, Comer B, Scheiderer B, Imhoff FB, Morikawa D, Kia C, et al. The Effect of glenohumeral fixation angle on deltoid function during superior capsule reconstruction: a biomechanical investigation. Arthroscopy 2020;36:400–8.
[23] Berthold DP, Bell R, Muench LN, Jimenez AE, Cote MP, Obopilwe E, et al. A new approach to superior capsular reconstruction with hamstring allograft for irreparable posterosuperior rotator cuff tears: a dynamic biomechanical evaluation. J Shoulder Elbow Surg 2021;30:S38–s47.
[24] Berthold DP, Muench LN, Bell R, Uyeki C, Zenon K, Mazzocca AD, et al. Biomechanical consequences of isolated, massive and irreparable posterosuperior rotator cuff tears on the glenohumeral joint a dynamic biomechanical investigation of rotator cuff tears. Obere Extrem Schulter Ellenb Hand 2021;16:120–9.
[25] Berthold DP, Muench LN, Dyrna F, Scheiderer B, Obopilwe E, Cote MP, et al. Comparison of different fixation techniques of the long head of the biceps tendon in superior capsule reconstruction for irreparable posterosuperior rotator cuff tears: a dynamic biomechanical evaluation. Am J Sports Med 2021;49:305–13.
[26] Dyrna F, Berthold DP, Muench LN, Beitzel K, Kia C, Obopilwe E, et al. Graft tensioning in superior capsular reconstruction improves glenohumeral joint kinematics in massive irreparable rotator cuff tears: a biomechanical study of the influence of superior capsular reconstruction on dynamic shoulder abduction. Orthop J Sports Med 2020;8:2325967120957424.
[27] Dyrna F, Kumar NS, Obopilwe E, Scheiderer B, Comer B, Nowak M, et al. Relationship between deltoid and rotator cuff muscles during dynamic shoulder abduction: a biomechanical study of rotator cuff tear progression. Am J Sports Med 2018;46:1919–26.
[28] Muench LN, Otto A, Kia C, Obopilwe E, Cote MP, Imhoff AB, et al. Rotational range of motion of elliptical and spherical heads in shoulder arthroplasty: a dynamic biomechanical evaluation. Arch Orthop Trauma Surg 2023:10.
[29] Scheiderer B, Kia C, Obopilwe E, Johnson JD, Cote MP, Imhoff FB, et al. Biomechanical effect of superior capsule reconstruction using a 3-mm and 6-mm thick acellular dermal allograft in a dynamic shoulder model. Arthroscopy 2020; 36:355–64.
[30] Gulotta LV, Choi D, Marinello P, Knutson Z, Lipman J, Wright T, et al. Humeral component retroversion in reverse total shoulder arthroplasty: a biomechanical study. J Shoulder Elbow Surg 2012;21:1121–7.
[31] Gulotta LV, Choi D, Marinello P, Wright T, Cordasco FA, Craig EV, et al. Anterior deltoid deficiency in reverse total shoulder replacement: a biomechanical study with cadavers. J Bone Joint Surg Br 2012;94:1666–9.
[32] Hansen ML, Otis JC, Johnson JS, Cordasco FA, Craig EV, Warren RF. Biomechanics of massive rotator cuff tears: implications for treatment. J Bone Joint Surg Am 2008;90:316–25.
[33] Scalise J, Jaczynski A, Jacofsky M. The effect of glenosphere diameter and eccentricity on deltoid power in reverse shoulder arthroplasty. Bone Joint J 2016; 98-b:218–23.
[34] Sharkey NA, Marder RA. The rotator cuff opposes superior translation of the humeral head. Am J Sports Med 1995;23:270–5.
[35] Sharkey NA, Marder RA, Hanson PB. The entire rotator cuff contributes to elevation of the arm. J Orthop Res 1994;12:699–708.
[36] Apreleva M, Hasselman CT, Debski RE, Fu FH, Woo SL, Warner JJ. A dynamic analysis of glenohumeral motion after simulated capsulolabral injury. A cadaver model. J Bone Joint Surg Am 1998;80:474–80.
[37] Debski RE, McMahon PJ, Thompson WO, Woo SL, Warner JJ, Fu FH. A new dynamic testing apparatus to study glenohumeral joint motion. J Biomech 1995; 28:869–74.
[38] Konrad GG, Jolly JT, Labriola JE, McMahon PJ, Debski RE. Thoracohumeral muscle activity alters glenohumeral joint biomechanics during active abduction. J Orthop Res 2006;24:748–56.
[39] Konrad GG, Markmiller M, Jolly JT, Ruter AE, Sudkamp NP, McMahon PJ, et al. Decreasing glenoid inclination improves function in shoulders with simulated massive rotator cuff tears. Clin Biomech 2006;21:942–9. Bristol, Avon.
[40] Konrad GG, Sudkamp NP, Kreuz PC, Jolly JT, McMahon PJ, Debski RE. Pectoralis major tendon transfers above or underneath the conjoint tendon in subscapularis-deficient shoulders. An *in vitro* biomechanical analysis. J Bone Joint Surg Am 2007; 89:2477–84.
[41] Labriola JE, Lee TQ, Debski RE, McMahon PJ. Stability and instability of the glenohumeral joint: the role of shoulder muscles. J Shoulder Elbow Surg 2005;14: 32s–8s.
[42] McMahon PJ, Debski RE, Thompson WO, Warner JJ, Fu FH, Woo SL. Shoulder muscle forces and tendon excursions during glenohumeral abduction in the scapular plane. J Shoulder Elbow Surg 1995;4:199–208.
[43] McMahon PJ, Eberly VC, Yang BY, Lee TQ. Effects of anteroinferior capsulolabral incision and resection on glenohumeral joint reaction force. J Rehabil Res Dev 2002;39:535–42.
[44] Parsons IM, Apreleva M, Fu FH, Woo SL. The effect of rotator cuff tears on reaction forces at the glenohumeral joint. J Orthop Res 2002;20:439–46.
[45] Thompson WO, Debski RE, Boardman ND, Taskiran E, Warner JJ, Fu FH, et al. A biomechanical analysis of rotator cuff deficiency in a cadaveric model. Am J Sports Med 1996;24:286–92.
[46] Hurschler C, Wülker N, Mendila M. The effect of negative intraarticular pressure and rotator cuff force on glenohumeral translation during simulated active elevation. Clin Biomech 2000;15:306–14. Bristol, Avon.
[47] Roetman B, Wuelker N, Plitz W. A dynamic shoulder model for biomechanical measurements of shoulder specimen. Biomed Tech 1996;41:359–63 (Berl).
[48] Wuelker N, Korell M, Thren K. Dynamic glenohumeral joint stability. J Shoulder Elbow Surg 1998;7:43–52.
[49] Wuelker N, Plitz W, Roetman B. Biomechanical data concerning the shoulder impingement syndrome. Clin Orthop Relat Res 1994:242–9.
[50] Wuelker N, Plitz W, Roetman B, Rossig S. Biomechanical investigation of the impingement syndrome at the shoulder. Z Orthop Ihre Grenzgeb 1995;133:61–6.
[51] Wuelker N, Plitz W, Roetman B, Wirth CJ. Function of the supraspinatus muscle. abduction of the humerus studied in cadavers. Acta Orthop Scand 1994;65:442–6.
[52] Wuelker N, Roetman B, Roessig S. Coracoacromial pressure recordings in a cadaveric model. J Shoulder Elbow Surg 1995;4:462–7.
[53] Wuelker N, Schmotzer H, Thren K, Korell M. Translation of the glenohumeral joint with simulated active elevation. Clin Orthop Relat Res 1994:193–200.
[54] Wuelker N, Wirth CJ, Plitz W, Roetman B. A dynamic shoulder model: reliability testing and muscle force study. J Biomech 1995;28:489–99.
[55] Wülker N, Thren K, Korell M, Kirsch L. Measurement of glenohumeral joint translation with a dynamic shoulder model. Z Orthop Ihre Grenzgeb 1996;134: 67–72.
[56] Payne LZ, Deng XH, Craig EV, Torzilli PA, Warren RF. The combined dynamic and static contributions to subacromial impingement. A biomechanical analysis. Am J Sports Med 1997;25:801–8.
[57] Giles JW, Ferreira LM, Athwal GS, Johnson JA. Development and performance evaluation of a multi-PID muscle loading driven *in vitro* active-motion shoulder simulator and application to assessing reverse total shoulder arthroplasty. J Biomech Eng 2014;136:121007.
[58] Giles JW, Ferreira LM, Athwal GS, Johnson JA. VALIDATION of a novel *in-vitro* simulator for real-time control of active shoulder movements in various planes of motion. New York: Amer Soc Mechanical Engineers; 2014.
[59] Giles JW, Langohr GD, Johnson JA, Athwal GS. Implant design variations in reverse total shoulder arthroplasty influence the required deltoid force and resultant joint load. Clin Orthop Relat Res 2015;473:3615–26.
[60] Giles JW, Langohr GD, Johnson JA, Athwal GS. The rotator cuff muscles are antagonists after reverse total shoulder arthroplasty. J Shoulder Elbow Surg 2016; 25:1592–600.
[61] Kedgley AE, Mackenzie GA, Ferreira LM, Drosdowech DS, King GJ, Faber KJ, et al. Humeral head translation decreases with muscle loading. J Shoulder Elbow Surg 2008;17:132–8.
[62] Kedgley AE, Mackenzie GA, Ferreira LM, Johnson JA, Faber KJ. *In vitro* kinematics of the shoulder following rotator cuff injury. Clin Biomech 2007;22:1068–73. Bristol, Avon.
[63] Kedgley AE, Shore BJ, Athwal GS, Johnson JA, Faber KJ. An in-vitro study of rotator cuff tear and repair kinematics using single- and double-row suture anchor fixation. Int J Shoulder Surg 2013;7:46–51.
[64] Langohr GD, Giles JW, Athwal GS, Johnson JA. The effect of glenosphere diameter in reverse shoulder arthroplasty on muscle force, joint load, and range of motion. J Shoulder Elbow Surg 2015;24:972–9.
[65] Wuelker N, Roetman B, Plitz W, Knop C. Function of the supraspinatus muscle in a dynamic shoulder model. Unfallchirurg 1994;97:308–13.
[66] Escamilla RF, Yamashiro K, Paulos L, Andrews JR. Shoulder muscle activity and function in common shoulder rehabilitation exercises. Sports Med 2009;39: 663–85.
[67] Kronberg MNG, Broström LA. Muscle activity and coordination in the normal shoulder. an electromyographic study. Clin Orthop Relat Res 1990;257:76–85.
[68] Giroux B, Lamontagne M. Net shoulder joint moment and muscular activity during light weight-handling at different displacements and frequencies. Ergonomics 1992;35:385–403.

[69] van der Helm FC, Veeger HE. Quasi-static analysis of muscle forces in the shoulder mechanism during wheelchair propulsion. J Biomech 1996;29:39–52.
[70] Veeger HE, van der Helm FC. Shoulder function: the perfect compromise between mobility and stability. J Biomech 2007;40:2119–29.
[71] Kian A, Pizzolato C, Halaki M, Ginn K, Lloyd D, Reed D, et al. Static optimization underestimates antagonist muscle activity at the glenohumeral joint: a musculoskeletal modeling study. J Biomech 2019;97:109348.
[72] Inman VT, Saunders JB, Abbott LC. Observations of the function of the shoulder joint. 1944 Clin Orthop Relat Res 1996:3–12.
[73] McQuade KJ, Smidt GL. Dynamic scapulohumeral rhythm: the effects of external resistance during elevation of the arm in the scapular plane. J Orthop Sports Phys Ther 1998;27:125–33.
[74] Zhang Q, Hosoda R, Venture G. Human joint motion estimation for electromyography (EMG)-based dynamic motion control. Annu Int Conf IEEE Eng Med Biol Soc 2013;2013:21–4.
[75] Chung SW, Park H, Kwon J, Choe GY, Kim SH, Oh JH. Effect of hypercholesterolemia on fatty infiltration and quality of tendon-to-bone healing in a rabbit model of a chronic rotator cuff tear: electrophysiological, biomechanical, and histological analyses. Am J Sports Med 2016;44:1153–64.